Electronic structure of self-assembled Ag nanowires on Si(557): spectroscopic evidence for dimensionality

2015 New J. Phys. 17 093025

(http://iopscience.iop.org/1367-2630/17/9/093025)

New Journal of Physics
The open access journal at the forefront of physics

Deutsche Physikalische Gesellschaft DPG
IOP Institute of Physics

Published in partnership with: Deutsche Physikalische Gesellschaft and the Institute of Physics

OPEN ACCESS

RECEIVED
30 June 2015

REVISED
6 August 2015

ACCEPTED FOR PUBLICATION
18 August 2015

PUBLISHED
16 September 2015

PAPER

Electronic structure of self-assembled Ag nanowires on Si(557): spectroscopic evidence for dimensionality

C W Nicholson[1], C Monney[2], U Krieg[3], C Tegenkamp[3], H Pfnür[3], K Horn[1] and M Wolf[1]

[1] Department of Physical Chemistry, Fritz-Haber-Institut of the Max Planck Society, Faradayweg 4-6, D-14915 Berlin, Germany
[2] Institute of Physics, University of Zurich, Winterthurerstrasse 190, 8057 Zurich, Switzerland
[3] Institut für Festkörperphysik, Leibniz Universität, Appelstraß e 2, Hannover, Germany

E-mail: nicholson@fhi-berlin.mpg.de

Keywords: dimensionality, electronic structure, vicinal Si surface, doping, 1D confining potential

Abstract

We investigate the electronic structure of silver nanowires at 1 monolayer (ML) Ag coverage on a vicinal Si(557) substrate by angle-resolved photoemission spectroscopy. Fermi surface mapping reveals two-dimensional (2D) Ag-induced electron pockets, which shift to higher binding energies by n-type doping of the step edges. The electronic structure of the 1 ML Ag/Si(557) system exhibits additional 2D metallic states near the Fermi level, which may originate from substrate induced periodicities. By considering the confining potential and electronic coherence length we reconcile the seemingly conflicting views of the dimensionality in this system probed by photoemission spectroscopy, and the dispersion of collective excitations as detected by electron energy loss spectroscopy .

Introduction

Control of the electronic properties in nanoscale structures is an area of both fundamental and technological importance. By confining electrons to low dimensions it is possible to induce a variety of phenomena resulting from increased electronic interactions and quantum effects. This is manifested in the observation of, for example, spin and charge density waves [1, 2], metallic quantum well states [3], metallic two-dimensional (2D) electron gases on the surface of bulk insulating oxides [4, 5], relativistic Dirac fermions and edge states in graphene [6], topological surface states [7], and Majorana fermions [8].

Metal wires on semiconducting substrates are important model systems for low dimensional materials. Not only do some of these systems exhibit well defined quasi-one-dimensional (1D) metallic band structures [9, 10] but through variation of parameters such as the terrace width or by doping, a degree of control over electronic confinement and interactions may be achievable which is difficult to obtain with bulk 1D crystals such as $NbSe_3$ or the Bechgaard salts [11]. An examination of electronic states at the Fermi level reveals the degree to which a system can be considered to be electronically 1D, and probes the effects that arise from electronic localization and coupling to the bulk environment of the substrate.

Ag on the Si(557) surface at coverages around 0.3 monolayer (ML) (with respect to Si(111) surface atom density i.e. 1 ML $= 7.83\times10^{14}$ cm^{-2}) forms atomic nanowires, however angle-resolved photoemission spectroscopy (ARPES), electron energy loss spectroscopy (EELS) and scanning tunneling spectroscopy all show that these wires are semiconducting [12, 13]. More recent work has focused on Ag/Si(557) wires at a coverage of 1 ML of Ag [13, 14]. Unlike the 0.3 ML atomic wires, at these higher coverages Ag forms a $\sqrt{3}$ structure, as on the Si(111) surface, but with a clear real space anisotropy induced by the stepped Si(557) surface. A strong anisotropy in the plasmon dispersion observed along and across these wires has been interpreted as evidence for quasi-1D metallic behaviour. These collective excitations occur beyond coverages of 0.3 ML, where the $\sqrt{3}$ structure starts to form, and their emergence was assigned to electron doping by Ag atoms or residual gas [14] which populates the Ag-induced bands and shifts them below the Fermi level in a similar way to that observed on the Ag/Si(111) surface [15]. The clean, stoichiometric 1 ML Ag/Si(557) surface is thought to be semiconducting, only becoming metallic upon doping.

These observations call for an investigation of the momentum-resolved valence level structure; in particular near the Fermi level. We study this system using ARPES, starting with the doping induced transition to the

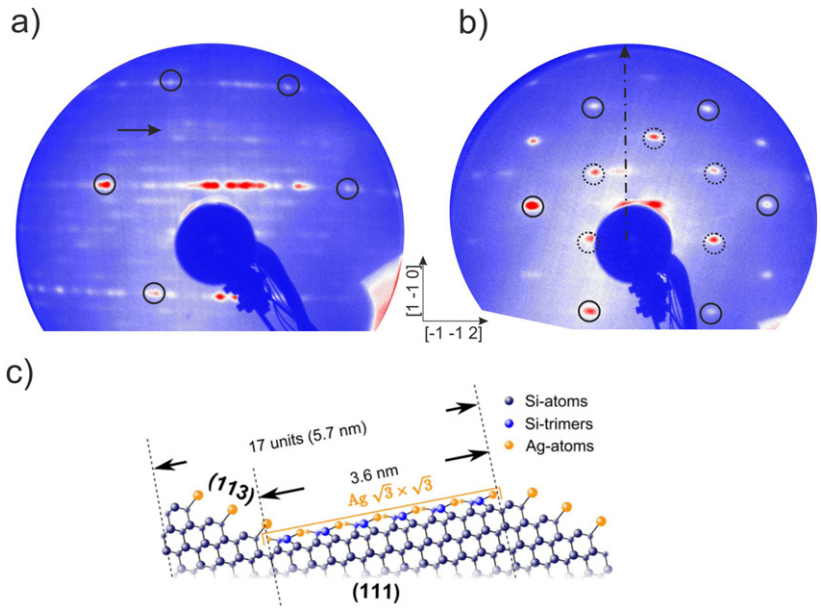

Figure 1. (a) LEED image of the clean Si(557); circles highlight the 1×1 structure and the arrow marks the (weak) $\times 2$ intensity produced by period doubling along the step edge, indicative of high quality surface preparation. (b) 1 ML Ag on Si(557). Solid circles mark 1×1 structure as in (a) and dotted circles mark the $\sqrt{3}$ spots. Both images were taken with 77 eV electron beam. The dashed–dotted arrow marks the line cut position along the wire (see figure 4 and text). (c) Schematic representation of the 1 ML Ag/Si(557) structure, from [18].

metallic Ag/Si(557) 'nanowire' structure. We then examine the features at the Fermi level induced by the terrace/step edge superstructure by comparing the Fermi surface of the flat $\sqrt{3} \times \sqrt{3}$ R30°Ag/Si(111) surface with that of the 1 ML Ag/Si(557).

Experimental

As a basis for the preparation of the 1 ML Ag/Si(557) nanowire structure, a non-faceted Si(557) surface is used as a template. Si(557) n-type crystals were outgassed at 500 °C for many hours followed by a flashing procedure to 1200 °C. The base pressure in the chamber was 5×10^{-10} mbar, and was never higher than 1.2×10^{-9} mbar during flashing. The quality of the substrate preparation was confirmed by LEED. Ag was evaporated at a rate of around 0.05 ML/min with the Si substrate held at room temperature. The sample was then annealed at 500 °C for 10 min to induce the $\sqrt{3}$ structure. Note that this procedure differs slightly from previous work [13, 14], where Ag deposition was performed at 500 °C. LEED images of the clean Si(557) and $\sqrt{3}$ Ag nanowires are shown in figures 1(a) and (b). The evaporator was calibrated using the LEED phase diagram of Ag/Si(111) and Ag/Si(557) [13, 16]. Ag/Si(557) is composed of a (111) terrace 3.6 nm wide and step edges with a (113) orientation as shown in figure 1(c). The size of one full unit is 5.7 nm. After preparation the sample was transferred to a liquid N_2 cooled manipulator in a chamber with a base pressure of 3×10^{-11} mbar when cold. ARPES and XPS measurements were carried out on the UE56-PGM1 beam line at BESSY II (Berlin) with an end station employing a SPECS PHOIBOS100 electron analyser. Linear horizontally polarized radiation at a photon energy of 112 eV was used, as this maximized the ARPES signal of bands close to the Fermi level. Fermi surface mapping was carried out at 100 K.

Results

Doping effects observed in the band structure

The valence band features as measured by ARPES of a freshly prepared 1 ML Ag/Si(557) surface (which includes around 20 mins. exposure to residual gas during which time LEED and transfer to the measurement chamber are carried out) and one which has acquired a considerable n-type doping are shown in figures 2(a) and (b). The data are normalized to the sum of the energy distribution curves (EDCs) in order to highlight features near the Fermi level. In the undoped case, emission from the Si-derived bands is observed at normal emission ($k_{||} = 0$) and a binding energy below 0.3 eV. A small electron pocket just below the Fermi level is observed at 1.15 Å^{-1}, which is shifted down towards higher binding energies over the course of a few hours until a parabolic band is seen as

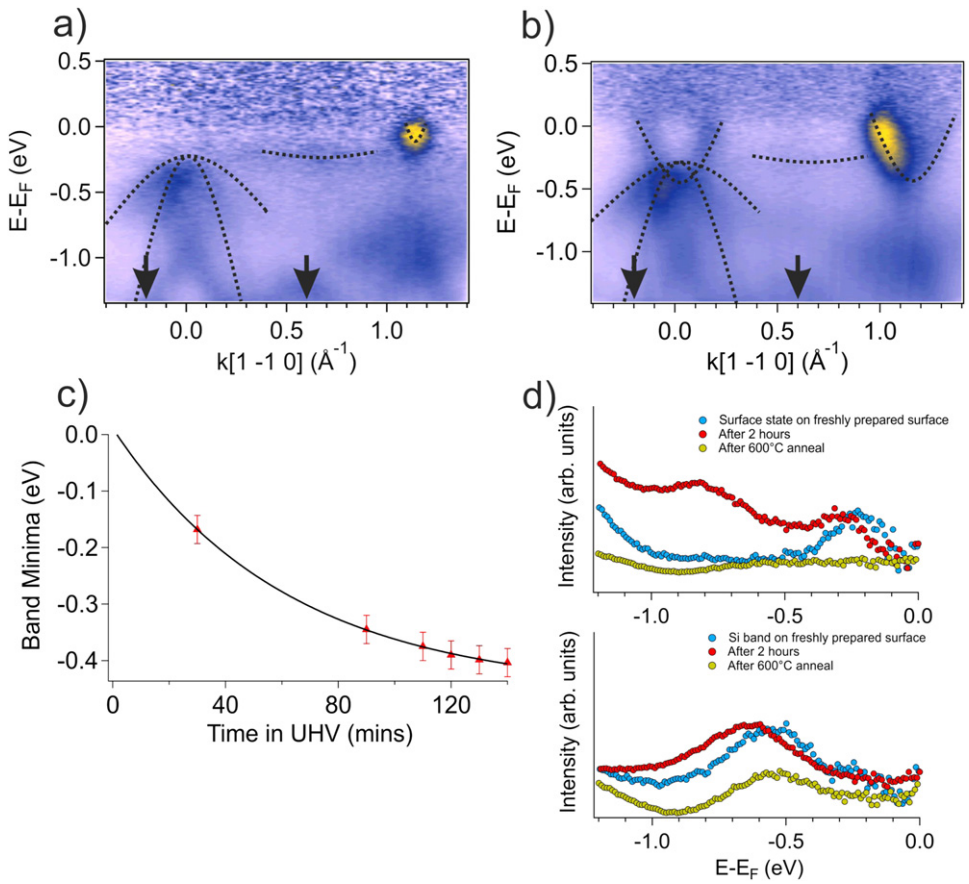

Figure 2. (a) Photoemission image of valence band states recorded with a photon energy of 112 eV from an freshly prepared sample showing only a very small electron pocket below the Fermi level at $k_{||}$. States from the Si substrate are also highlighted. (b) Same sample after 2 h in residual gas pressure of 5×10^{-11} mbar showing well developed bands. Dotted lines are a guide to the eye. (c) Shift of band minima at 1.15 Å^{-1} as a function of time in residual gas. (d) EDCs of figures (a) and (b) at 0.6 Å^{-1}($\pm$ 0.15 Å^{-1} integration window) revealing the peak at 220 meV below E_F assigned to atoms bonded to the (113) step edges. The position of the Si bands at $k\,[1-10] = -0.2$ Å^{-1} is shown in the lower panel. Both surface and Si bands undergo a 80 meV shift in the time it takes to dope the Ag bands. Arrows in (a) and (b) mark the fixed k positions at which EDCs are obtained.

shown in figure 2(b). An electron pocket at normal emission is now also evident. The intensity distribution of the pocket resulting in half of the band appearing much brighter than the other is caused by matrix element effects which are further revealed by the full Fermi surface presented below. During the time between the two data sets, no additional material was introduced to the system; hence we assign the changes to residual gas adsorption. The appearance of a pocket already in the freshly prepared sample is likely a result of residual gas absorption during the time taken to check the preparation with LEED and transfer to the measurement chamber. Thus it is likely that the true 1 ML surface is semiconducting. Figure 2(c) summarizes the band position dynamics, obtained by extracting the minima of the band[4] at 1.15 Å^{-1} which is shifted by 250 meV over a period of around 2 h. This time scale is consistent with the EELS study on this system [14] which also reveals residual gas doping of the system. The Si bands from the substrate also shift during this time, but only by 80 meV (see figure 2(d)), most likely due to surface photo voltage induced band bending. No change was observed in the LEED pattern of the sample, other than a broadening of spots due to reduced surface quality, hence a surface reconstruction can be ruled out as the cause of this shift. Quantitatively similar residual gas induced shifts were also found on the Ag/Si(111) surface [17].

We find that doping by residual gas is accompanied by a small uptake of oxygen, as measured with XPS[5] (not shown here). Previous work has shown that Ag may also be used to dope the semiconducting 1 ML Ag/Si system

[4] Band positions were extracted by fitting the momentum distribution curves with Lorentzian peaks and a constant background. A parabolic distribution was then fitted to the band position in order to obtain the energy minima.

[5] Based on our data we infer that Ag doping may require the surface to have already absorbed some critical amount of residual gas. Most likely this finding, which differs from previous work, results from the subtle differences in preparation: whether the sample is annealed during or after Ag evaporation. Annealing leads to a locally increased pressure close to the sample, and XPS data shows that the surface oxygen 1 s peak increases after annealing. In addition, the presence of Ag on the surface will reduce the uptake of residual gas during the post-anneal. Residual gas absorption on the bare Si(557) surface has been found to strongly influence the growth of Ag into nanowires or islands and may play a role in this system. Such an effect is likely stronger on the Si(557) surface compared with the Si(111) surface due to the increased sticking probability of impurities at step edges compared with a flat surface.

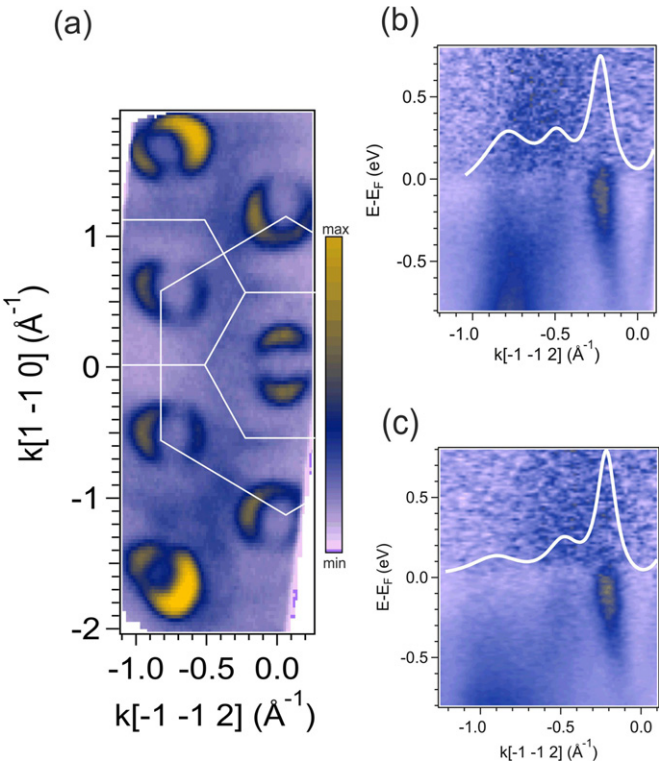

Figure 3. (a) Fermi surface of Ag/Si(557) taken with 112 eV photon energy. The matrix element effect which produces regions of missing intensity is clearly visible. The Brillouin zones of the (111) and $\sqrt{3}$ (smaller hexagons) surfaces are overlaid in white. A slight uncorrected distortion due to misalignment causes the pockets towards the edge of the image to appear non-circular. (b) Cut in energy and momentum through the Fermi surface along $[-1\ -1\ 2]$ (perpendicular to the wire direction) at -1.3 Å^{-1} in (a). Two dispersing states are observed, which are assigned as the Ag/Si(111) surface state at the $\sqrt{3}$ Brillouin zone centre and a replica of this. (c) Energy and momentum cut along $[-1\ -1\ 2]$ at 1.3 Å^{-1}. The white curves are fits to the MDC spectra in a 100 meV window around the Fermi level.

into the metallic phase [14, 15]. Previous XPS work on the Ag/Si surface exposed to oxygen has found additional components of the O 1 s peak, which are interpreted as surface absorbed or sub-surface oxygen [19]. A more recent study suggested oxygen related species can bind at elevated pressure at steps on a metallic Ag surface [20], which may be relevant in the present vicinal system. However a detailed understanding of the reaction mechanism is beyond the scope of this study.

An additional electronic band is found at 220 meV below E_F with the minimum in energy centred at 0.6 Å^{-1} in figures 2(a) and (b). EDCs around this value are presented in figure 2(d). Annealing the sample to 600 °C for 15 s removes this state, while retaining around 90% of the surface Ag [14]; we hence assign this feature to a surface state. This state may be the signature of (residual gas) atoms weakly bonded to the step edges which extrinsically dope the Ag states on the (111) terraces as proposed in a recent study [18]. This model additionally predicts a band bending induced by the charges absorbed at the step edges. As previously described, we observe a rigid band shift of 80 meV during the time in which the Ag pocket is doped into the metallic phase, which we attribute to a band bending effect. Our data appear consistent with the proposed extrinsic doping model.

Ag nanowire electronic structure

In order to better understand the electronic structure arising from the vicinal substrate interaction with the Ag layer, it is useful to first consider that of the Ag/Si(111) system. A schematic of the (111) and $\sqrt{3}$ Brillouin zones is overlaid in figure 3(a). The Ag/Si(111) Fermi surface has hexagonal symmetry, with an Ag-induced electron pocket appearing at each of the K-points of the (111) Brillouin zone, which are the Γ -points of the $\sqrt{3}$ reconstructed Brillouin zone [21]. Thus only Ag states contribute to the Fermi surface. These pockets have parabolic dispersion below the Fermi level (E_F). The pockets are circular in the $k_x k_y$ plane, but each has a notch of intensity removed, the exact position of which depends on the energy and polarization of light incident on the sample. Such a 'dark corridor' effect in the photoemission intensity is reminiscent to that observed on graphene due to the Berry phase [22].

A similar result is obtained on the Ag/Si(557) surface for a fully doped system, as described in the previous section. Figure 3(a) shows an overview of the Fermi surface, which shows the same electron pockets at the $\sqrt{3}$

Brillouin zone centres as on the Ag/Si(111) surface. The position of normal emission is rotated by 9° compared with that of a flat (111) surface, corresponding to the miscut direction required to produce the vicinal Si(557) surface. The measurement presented here is from the second Brillouin zone with the scale referenced to the centre of the zone.

In addition to the Ag-induced features from the Si(111) surface, intensity at the Fermi level is observed between the Ag pockets in the nanowire structure. These weak features have a circular intensity distribution and generally appear similar to the (111) Ag states. The energy versus momentum behaviour of these additional features is displayed in figures 3(b) and (c). Electron states are seen to disperse towards E_F in a parabolic fashion. Despite being weaker in intensity and sitting on top of a larger background the similarity to the (111) states is clear. These observations were reproduced on different substrates prepared on different days.

As is evident from the position of the replica bands, these states are shifted in momentum along both the [−1 −1 2] and the [1−1 0] azimuths. The value of the shifts are extracted by analysis of line cuts through the Fermi surface along the two azimuths as presented in figures 4 (a) and (b). Along the [−1 −1 2] direction we obtain a shift vector of 0.15 $Å^{-1}$ while parallel to the wires along [1−1 0] we obtain 0.38 $Å^{-1}$.

In order to further confirm these as shifted replica states, figure 3(a) is represented with a different colour scheme and changed contrast as figure 4(d). This image clearly reveals a number of circular replica pockets, additional to the pockets found on the Ag/Si(111) Fermi surface.

Perpendicular to the nanowires the Umklapp vector of 0.15 $Å^{-1}$ corresponds closely to the value expected for the interwire distance resulting from the 5.7 nm periodicity. This suggests some amount of inter-wire coupling exists in this system. However considering the very weak intensity of these replicas compared with the main electronic states, we would interpret this to mean that such coupling is very weak. A similar scenario is observed in Pb/Si(557) nanowires [28], or on Cu and Au vicinal surfaces [26]. As will be discussed further below, the short electronic coherence length in this sample means that inter-wire coupling must be low.

The value of 0.38 $Å^{-1}$ is very close to 1/3 of the $\sqrt{3}$ Brillouin zone size of 1.1 $Å^{-1}$. Our LEED data also reveals a 1/3 periodicity as presented in the line cut figure 4(c). Thus is suggestive of a real space super-periodicity along the [1–1 0] direction i.e. along the wires. STM work on this system has shown the step edges display a characteristic triangular roughness [13] which results in a 'zig-zag' structure due to the $\sqrt{3} \times \sqrt{3}$ structure formed by Ag on the Si(111) terraces. Such a periodic modulation may be responsible for the shift of the Ag replica along the [1–1 0] azimuth via the transfer of a reciprocal lattice vector. However, it can be difficult to directly match this periodicity with that observed in the STM, as the exact nature of the step edges depends on the preparation and varies from sample to sample.

A sharp feature in ARPES additionally requires structural homogeneity on the length scale of the probing light beam, because of the incoherent superposition of spectral features from the sampled region. However, due to the roughness of the step edges as imaged by STM [13], replica features are strongly smeared out as clearly observed in our data.

A schematic of the Ag/Si(557) Fermi surface is presented in figure 4(e).

Discussion

This brings us to the discussion of the relation between the strong anisotropy in the plasmon dispersion along and across the wires seen by EELS [13], suggesting a 1D confined behaviour of collective electronic excitations, and the electronic band structure of the $\sqrt{3} \times \sqrt{3}$ terrace structures as revealed by ARPES, which appears to be dominated by features stemming from a 2D electronic structure.

These seemingly contradictory observations go to the heart of what it means for a system to be considered as 1D or 2D and raises the question: What is the relevant spatial scale probed by different experimental methods?

An important point is that there is a conceptual difference between 1D behaviour of collective excitations, and the dimensionality of metal-induced electronic surface states: the 1D behaviour of collective excitations as observed by EELS does not imply that the electron quasi-particles on the terraces themselves experience a 1D potential. Indeed we find no evidence for either 1D dispersion, or quantum confined states in our ARPES data. One of the regular applications of ARPES is to identify two-or three-dimensional extended (Bloch) states. Such extended systems may give rise to very sharp intrinsic line-widths in photoemission as in Cu(111) [35]. Additionally, confined states perpendicular to the step edges in terraces as large as 5.6 nm in Au(23 23 21) are observed in ARPES [34]. This implies that the reason we do not observe quantized states is not due to a limitation of the ARPES measurement itself, but rather it is an intrinsic property of Ag/Si(557).

A key concept in such systems is the potential barrier experienced by electrons at a step, calculated within a 1D Kronig–Penney model. For rather weak edge potentials electrons may propagate across many steps, resulting

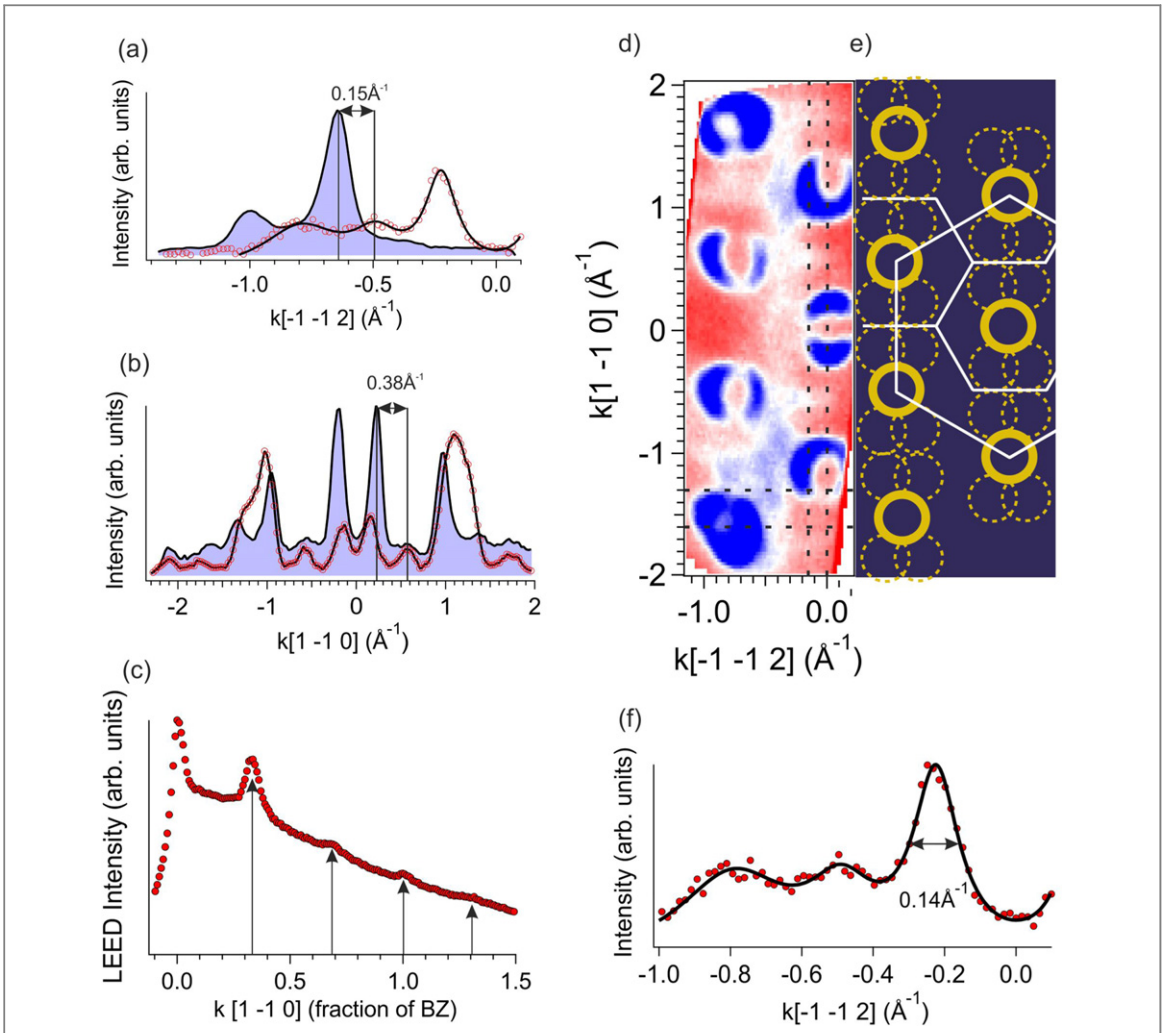

Figure 4. (a) Cuts through the Fermi surface shown in figure 3 along the [−1 −1 2] direction at −1.6 Å^{-1} through the Ag pockets (solid blue curve) and at at −1.3 Å^{-1} through the replica state (×10) (red dots and black fit curve) revealing an offset in momentum. (b) Cuts along the [1–1 0] direction. Blue filled curve taken at 0 Å^{-1} through the Ag pockets, red dots and black fit at −0.15 Å^{-1} centred on the replica states. Positions of cuts are shown in (d). (c) Cut through the LEED image of figure 1(b) revealing a 1/3 (0.4 Å^{-1}) (±0.025 Å^{-1}) periodicity along the wire direction. (d) Fermi surface as in figure 3(a), with a colour scale chosen to highlight the replica pockets and a schematic Fermi surface showing the replicas (dotted circles) and the pockets that are the same as the Ag/Si(111) Fermi surface (full circles). Dotted lines show the position of line cuts made in figures 3(a) and (b). (e) Schematic Fermi surface for Ag/Si(557). States which are the same as on the Ag/Si(111) Fermi surface are shown as solid yellow circles, while replica states are presented as dotted circles. (f) MDC at the Fermi level as in figure 3(b). The FWHM as extracted from a 4 Lorentzian fit is shown; from this the coherence length is estimated (see text).

in superlattice replicas spaced by the step periodicity, while a strong potential confines electrons to a single terrace resulting in quantum well states appearing perpendicular to the step potential. At intermediate values of the step potential as in Au(887) it is possible to observe both effects simultaneously such that one observes a superlattice replica with band gaps due to 1D confined quantum well levels. In Ag/Si(557) we observe clear replicas, but no signatures of quantum confined states. This implies the strength of the edge potentials is rather low. It is possible, however, that any confined state behaviour is obscured by the structural inhomogeneity of the nanowires. The edge potential should be rather homogeneous in order to produce a coherent signal—a variation in terrace width has been seen to contribute to the apparent 2D dispersion in photoemission from Cu(443) and Cu(665) [27]. From a structural point of view the Ag/Si(557) nanowires exhibit a considerable edge roughening, as imaged by the STM data in figure 3 of [13], which may broaden spectral features in ARPES and hide evidence of a gap opening. Thus it is possible that confined states exist, but are not resolved in our measurements. This would be consistent with potential barriers of the order $U_0 b = 2 - 3$ eV Å, as in Au(887) and Cu(10 10 11) or even 10 eV Å, as in Au(23 23 21). Unfortunately the lack of clear band gaps due to confined states, or a suitable flat surface reference state prevents us from extracting the absolute step potential in our data. However, by fitting the dispersion of the band at the Fermi level with a parabola and extracting the effective mass we are able to

estimate the step potential[6]. We estimated a value of $U_0 b = 5$ eV Å for the step potential. As a comparison, micro-conductivity measurements at the Ag/Si(111) surface found a potential of $U_0 b = 10$ eV Å at a single atomic step [36]. Our estimated value is consistent with a system in which superlattice replicas and quantum confined states coexist. The fact that we do not observe any quantum confined states may be the result of the step edge roughness as described above.

A second important quantity that should be considered is the electronic coherence length. This length is related in part to the number of defects or adsorbates on the surface, which act as scattering centres for electrons, and is reflected in the linewidth of a photoemission signal. This is particularly important in hetero-systems of metals on a semiconducting substrate where surface electrons are more effectively confined to 2D than at the surface of a metal single crystal, in which electrons may also be scattered perpendicular to the surface. The possibility of scattering into the bulk results in a small probability amplitude for back-scattering signal hence such features on noble metal surfaces are often rather weak, despite the fact that the coherence lengths are very long. We extract the intrinsic linewidth of the Ag states from our data, by fitting the momentum distribution curve at E_F along [−1−1 2] with Lorentzians in order to extract the width of the curve. The MDC and Lorentzian fit are presented in figure 4(f). From this analysis we estimate a value of 6 nm for the coherence length. This value implies that rather weak inter-wire interactions are possible, consistent with our observation of weak replica states. In a closely related system, Pb/Si(557), which has much shorter terrace widths, multiple replicas at the Fermi level are observed [28]. The stronger signal compared with that observed in our data suggests a larger back-scattered probability due to the electrons being able to propagate over, and interact with, multiple steps due to the shorter terrace width.

The fact that confined plasmon states are observed by EELS suggests that the confining potential is stronger for plasmons than it is for electrons. It is not straightforward to make a quantitative comparison between the scattering behaviour of single particle excitations, as observed in ARPES, and collective plasmon excitations, due to the different decay mechanisms i.e. recombination for single particle excitations and generation of electron hole pairs for plasmons. It is clear, however, that at these long wavelengths the step edges act as strong reflectors for plasmons so that standing waves across individual terraces can be detected by EELS.

A plasmon is a collective property of the electron gas. By virtue of being collective, such an excitation causes displacement of all electrons involved (within the coherence length of this excitation). If the excitation is confined to a region of the order or smaller than its own wavelength e.g. in a nanoparticle or perpendicular to a nanowire, all electrons participate in the excitation. A simple estimate of the surface plasmon wavelength from EELS data for the Ag/Si(557) nanowires provides a value around 3 nm: very comparable to the terrace width[7]. Thus the collective mode extends throughout the entire terrace. Due to their comparatively long wavelength, plasmons are less sensitive to atomistic defects, and may not strongly experience the edge roughening intrinsic to this system, thus experiencing only the averaged step potential. This may explain why confined states are observed in EELS, and not in ARPES.

It is interesting to consider the related features of other nanowire systems since these considerations are clearly more generally applicable.

ARPES clearly observes 1D features in the electron density induced by well separated single atomic chains as in the (4×1) reconstruction of In/Si(111), Au/Si(557), or by double chains in Au/Si(553) and Au/Si(775) [9, 24]. Another similar surface, the 5×2-Au/Si(111), reveals an unusual continuous 1D to 2D transition in a surface electron band, with a Peierls gap at the Fermi level [39]. However, a very different situation arises for Pb/Si(557) close to 1 ML coverage. Due to uncovered step edges, this structure still consists of well separated mini-terraces, but the ARPES signal is already essentially 2D, with a substrate mediated interaction producing replica states at the Fermi level [23, 28]. Only within 50 meV below E_F does a quasi-1D band gap become visible [29]. The step potential was estimated for this system as 60 meV [28], which implies a rather weak potential.

Plasmonic excitations measured by EELS, as in Ag/Si(557), reveal quantized effects suggestive of quasi-1D character [13, 25]. One explanation for the anisotropic plasmon dispersion, suggested by time-dependent density functional theory, assumes that a single dipole field confined to a terrace leads to quantized energy states of the plasmon oscillations across the wire direction [31, 32]. This would result in discrete energy losses perpendicular to the wires as found in a number of systems, including Ag/Si(557) [13, 25, 38]. However no such confined states are found on the (4×1)-In/Si(111) or Au/Si(557) systems, which implies these atomically narrow chains are unable to support collective oscillations perpendicular to the chain.

[6] In the tight-binding limit of the Kronig–Penney model $E = 2J(1 - \cos(ka))$ where $J = \pi^2\hbar^2/2m^2a^3U_0$, where a is the interwire distance. By approximating a parabolic dispersion near the bottom of a sinusoidal band such that $\cos(ka) \approx 1 - (ka)^2/2$ this allows us to write $m^* = m^2aU_0/2\pi^2\hbar^2$ by comparison to a free electron dispersion and hence estimate U_0.

[7] From the previously published EELS data it is known that plasmons disperse up to 0.19 Å^{-1} along the [1−1 0] direction. This corresponds to a real space value of 3.3 nm which results in the quantization of states along [−1 −1 2]. Hence using the plasmonic losses along [−1 −1 2] is not appropriate for determining the wavelength of the dispersing plasmons.

Summary

The Fermi surface of the 1 ML Ag/Si(557) 'nanowire' structure exhibits a small metallic pocket at the Brillouin zone boundary as observed by angle-resolved photoemission. This is likely the result of residual gas doping of the surface. Filling this band by electron doping moves it to higher binding energies by several hundred meV. We find evidence of a surface state which supports the existence of step-edge bound residual gas atoms which dope the Ag states on the (111) terraces, supporting a previously suggested extrinsic doping mechanism. In the fully doped phase we observe replicas of 2D Ag pockets which we suggest may result from an interaction with the anisotropic substrate which underlies the Ag phase.

By our analysis of the confining step potential, and the differing sensitivity of EELS and ARPES to disorder, we reconcile the apparent discrepancy between EELS and ARPES data in this quasi-1D system. Such considerations will be important when considering the application of low dimensional systems to device design.

Acknowledgments

We are grateful to H Vita and S Böttcher for technical advice, and we acknowledge financial support from the Deutsche Forschungsgemeinschaft (Grant No. FOR1700).

References

[1] Grüner G 1988 *Rev. Mod. Phys.* **60** 1129–81
[2] Grü G 1994 *Rev. Mod. Phys.* **66** 1–24
[3] Chiang T-C 2000 *Surf. Sci. Rep.* **39** 181
[4] Santander-Syro A F *et al* 2011 *Nature* **469** 189
[5] Meevasana W *et al* 2011 *Nat. Mater.* **10** 114
[6] Castro Neto A H, Guinea F, Peres N M R, Novoselov K S and Geim A K 2009 *Rev. Mod. Phys.* **81** 109
[7] Hasan M Z and Kane C L 2010 *Rev. Mod. Phys.* **82** 3045
[8] Nadj-Perge N *et al* 2014 *Science* **346** 602
[9] Crain J N *et al* 2004 *Phys. Rev.* B **69** 125401
[10] Sun Y J *et al* 2008 *Phys. Rev.* B **77** 125115
[11] Monceau P 2012 *Adv. Phys.* **61** 325
[12] Morikawa H *et al* 2008 *Surf. Sci.* **602** 3745
[13] Krieg U *et al* 2013 *J. Phys.: Condens. Matter* **25** 014013
[14] Krieg U *et al* 2014 *New J. Phys.* **16** 043007
[15] Crain J N *et al* 2005 *Phys. Rev.* B **72** 045312
[16] Wan K J *et al* 1993 *Phys. Rev.* B **47** 13700
[17] Johansson L S O *et al* 1989 *Phys. Rev. Lett.* **63** 2092
[18] Krieg U *et al* 2015 *New J. Phys.* **17** 043062
[19] Joyner R W and Roberts M W 1979 *Chem. Phys. Lett.* **60** 459
[20] Rocha T C R *et al* 2012 *Phys. Chem. Chem. Phys.* **14** 4554
[21] Crain J N *et al* 2002 *Phys. Rev.* B **66** 205302
[22] Liu Y *et al* 2011 *Phys. Rev. Lett.* **107** 166803
[23] Tegenkamp C *et al* 2005 *Phys. Rev. Lett.* **95** 176804
[24] Yeom H W *et al* 1999 *Phys. Rev. Lett.* **82** 4898
[25] Block T *et al* 2011 *Phys. Rev.* B **84** 205402
[26] Baumberger F *et al* 2004 *Phys. Rev. Lett.* **92** 016803
[27] Baumberger F *et al* 2004 *Phys. Rev. Lett.* **92** 196805
[28] Kim K S *et al* 2007 *Phys. Rev. Lett.* **99** 196804
[29] Tegenkamp C *et al* 2008 *Phys. Rev. Lett.* **100** 076802
[30] Krieg U 2014 1D-plasmonen in Ag-nanodrähten auf vicinalem Si(557) *Doctoral Thesis* Gottfried Wilhelm Leibniz Universität, Hannover
[31] Inaoka T 2005 *Phys. Rev.* B **71** 115305
[32] Yan J and Gao S 2008 *Phys. Rev.* B **78** 235413
[33] Temirov R *et al* 2006 *Nature* **444** 350
[34] Mugarza A *et al* 2002 *Phys. Rev.* B **66** 245419
[35] Tamai A *et al* 2013 *Phys. Rev.* B **87** 075113
[36] Matsudo I *et al* 2004 *Phys. Rev. Lett.* **93** 236801
[37] Friedrichowski S and Dumpich G 1998 *Phys. Rev.* B **58** 9689
[38] Ruderamigabo E P *et al* 2010 *Phys. Rev.* B **81** 165407
[39] Losio R *et al* 2000 *Phys. Rev. Lett.* **85** 808